

# Microscopic Frictional Response of Sodium Oleate Self-Assembled on Steel

Deepak Kumar · Sanjay Kumar Biswas

Received: 27 December 2007 / Accepted: 1 April 2008 / Published online: 15 April 2008  
© Springer Science+Business Media, LLC 2008

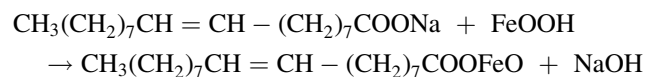
**Abstract** The article peruses the frictional response of an important metal working lubricant additive, sodium oleate. Frictional force microscopy is used to track the response of molecules self-assembled on a steel substrate of 3–4 nm roughness at 0% relative humidity. The friction-normal load characteristic emerges as bell-shaped, where the peak friction and normal load at peak friction are both sensitive to substrate roughness. The frictional response at loads lower than that associated with the peak friction is path reversible while at higher loads the loading and unloading paths are different. We suggest that a new low-friction interface material is created when the normal loads are high.

**Keywords** Tribology · Emulsifier · Steel · AFM

## 1 Introduction

Tribology of self-assembled organic monolayers have been studied extensively using lateral force microscopy [1–12], surface force apparatus [13–15], and molecular dynamics simulation [16–19]. Such studies have been motivated by the use of these monolayers as boundary lubricants in microelectromechanical systems (MEMS) [18], for machinery components [20] and artificial human joints [21]. These monolayers passivate reactive metal surfaces [22–24] and provide good load bearing support [24]. Nanotribological

studies of these monolayers have usually been done when they have been self-assembled monolayer (SAM) on functionalized ultra-smooth mica or silicon surfaces. The work reported here is motivated by the tribology of oil/water emulsions, used for cutting and shaping iron-based engineering components. The additives used in the emulsion have many functionalities such as; emulsification, friction modification and protection against oxidation and corrosion. As the metal is cut, the additives embedded in the trapped emulsion between the emerging chip and the rake face provide protection to the tool. Sodium oleate is a well-known cutting fluid additive of high hydrophilic-lipophilic balance (HLB) value of 18 [25]. Here we study the friction of sodium oleate self-assembled on an engineering steel surface, using lateral force microscopy. When sodium oleate is added to the oil as an emulsifier, the carboxylic group (–COONa) project out of the oil droplet [25]. When the droplet comes to the active contact zone it is likely to interact with the steel surface. When oxidized steel surface is exposed to a solution of sodium oleate ( $\text{CH}_3(\text{CH}_2)_7\text{CH} = \text{CH} - (\text{CH}_2)_7\text{COONa}$ ), an iron-oleate complex is formed [26].



When counterface asperities slide on a monolayer frictional resistance is experienced. Molecular dynamic simulation studies of the sliding process have suggested deformation modes of the molecules such as tilting and gauche defect generation. While only a limited [27] direct correlation has been attempted between mechanisms as suggested by the simulation studies and the experimental observations made in sliding of the SAM, such mechanisms have been invoked frequently to rationalize experimental observations. The latter suggests that with an increase in

D. Kumar · S. K. Biswas (✉)  
Department of mechanical engineering, Indian Institute of Science, Bangalore, Karnataka, India  
e-mail: skbis@mecheng.iisc.ernet.in

D. Kumar  
e-mail: dkumar@mecheng.iisc.ernet.in

contact loading there is an increase in gauche defect population [28, 29] as well as collective molecular tilt [5] towards the substrate. It is possible that when the load is sufficiently high the substrate comes to interact with a substantial part of the molecular chains.

If this happens the chains may lie almost parallel to the substrate with the normal load bearing upon the chain axis. The chain and the substrate atoms in the process may come close enough, to form chemical bonds between the monolayer and the substrate. Bowden and Tabor [30] showed that when a metal is dipped in a dilute solution of a fatty acid, the fatty acid chemisorbs on the metal surface and under sliding condition a metallic soap of the acid is formed. The soap has lubricating property. The authors show that when the solution concentration is sufficiently high even relatively passive metals such as iron and aluminum react with the fatty acid to form the lubricating soap.

In this article we explore the effect of load on the friction of sodium oleate SAM on steel. Self-assembly on an iron surface gives rise to an iron-oleate complex, at the head group level. The objective is to track the effect of increasing load on friction and to observe whether increasing the proximity of the chain to the substrate, by increasing the load, triggers a phase change in the monolayer.

## 2 Experimental

### 2.1 Materials and Sample Preparation

EN 31 steel is used as the substrate. Sodium oleate (Rohm and Haas Laboratory Reagent, Bombay, India) was used as received. n-hexane (99+%, anhydrous) (Sigma-Aldrich, USA) were used as organic solvent. Deionized water, obtained by processing of distilled water through millipore purification (Milli-Q, USA) system, was used to hydrolyze the substrate. Steel samples were polished mechanically (sequentially with a 1–3  $\mu\text{m}$  and a 0.25  $\mu\text{m}$  diamond paste) to obtain 3–4 nm rms (root mean square) roughness and were then sonicated with acetone for 15 min to remove all polishing debris. The polished samples were kept in air for 1 h to generate a natural oxide film on the substrate and were then sonicated with millipore water for 30 min. The substrates were flushed with a stream of dry nitrogen gas and were preserved in desiccators. Before deposition of SAM, samples were kept in ultraviolet (UV) cleaning chamber (Bioforce nanosciences, US) for 30 min to burn all carbonaceous contaminations, which block the adsorption sites. The steel samples prepared as above, were immersed in a freshly prepared sodium oleate solution (1 mM) for 20 h, taken out, rinsed and washed with

n-hexane (twice) followed by rinsing them with ethanol for 10 min to remove excess and physisorbed molecules.

### 2.2 FTIR Analysis

All spectra were taken by infrared reflection absorption spectroscopy (IRRAS) (GX spectrometer, Perkin Elmer, USA). The instrument is equipped with a liquid nitrogen cooled mercury cadmium telluride (MCT) detector. All IR spectra reported here are referenced to bare steel substrate over 1024 optimized scans at 4  $\text{cm}^{-1}$  resolution by using p-polarized beam. The sample and detector chambers were purged with nitrogen gas before starting the experiments and at regular intervals. A heating accessory (Harrick scientific corporation, New York, USA) was used for taking the spectra with an incident angle of 75° from the surface normal. The spectral analysis was carried out using spectrum 3.02 version software (Perkin-Elmer, USA).

### 2.3 Lateral Force Measurement

All AFM experiments were performed using an ‘‘EXPLORER’’ (Thermo Microscopes, Santa Barbara, USA) with  $\text{Si}_3\text{N}_4$  cantilevers (Thermo Microscope, CA, USA) associated with a pyramidal tip of nominal radius of 50 nm. The cantilever normal stiffness was found using thermal vibration technique, built into the software. A V-shaped cantilever of stiffness 0.15 N/m was used in all the experiments. All the tips were cleaned in an UV chamber for 20 min before experiments. Lateral force measurements were carried out in a 0% relative humidity established in a custom-made air-tight chamber. Ultra pure nitrogen gas, which contains 2 ppm water, was used to purge the chamber and generate 0% relative humidity. The experimental procedure comprised the tip approaching to contact, decreasing the load to  $-8$  nN and then recording friction as the load is increased to a maximum of 35–40 nN. The lateral force reported here [24], is the average of the difference in forces recorded in the forward and reverse scan. The lateral force was recorded using  $400 \times 400$  nm<sup>2</sup> scan area with different scan rates from 100 nm/s to 900 nm/s. The lateral force calibration method is reported elsewhere [24].

### 2.4 Nanotribometer

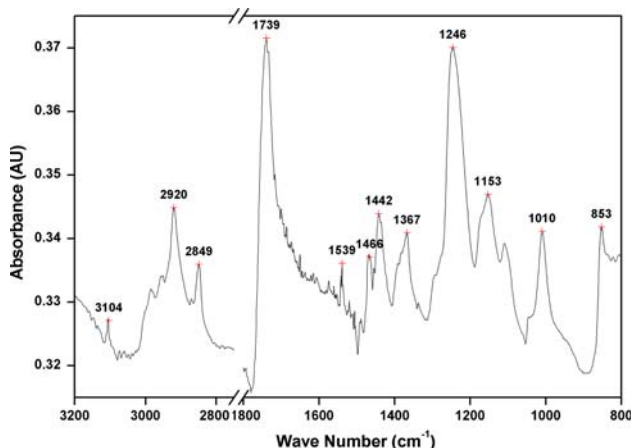
Tribological experiments were carried out in the 25–300 mN load range using a ball on disk tribometer (Nanotribometer, CSM Instruments, Switzerland). The ball used is of 100 Cr6 steel and has a diameter of 2 mm. The steel ball was cleaned with acetone in an ultrasonic bath prior to the experiment. Two sensing mirrors attached to the cantilever head (which carries the ball at one end),

perpendicular to each other (X and Z axis) measure displacements of the cantilever during sliding. During sliding, the friction coefficient is continuously calculated from measuring the X and Z displacements of the cantilever. All measurements were carried out under ambient conditions (relative humidity: 35%, temperature: 296 K), and under controlled relative humidity conditions at different sliding speed.

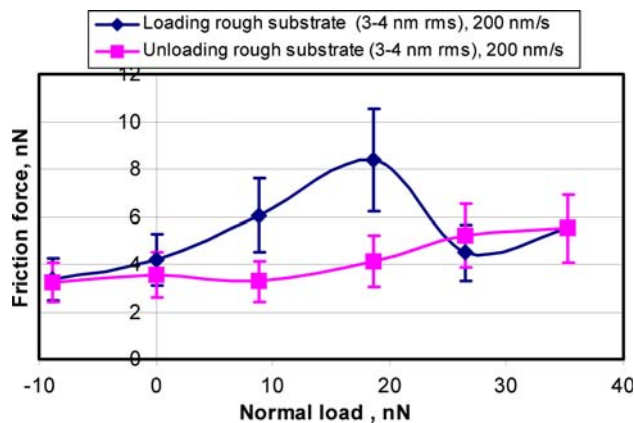
### 3 Results and Discussion

Figure 1 shows the IR spectra of SAM of sodium oleate adsorbed on a steel substrate of 3–4 nm rms (root mean square) roughness. It shows absorption bands at 2,920 and 2,849  $\text{cm}^{-1}$ , which arises from antisymmetric ( $d^-$ ) and symmetric ( $d^+$ ) methylene group stretching vibrations respectively, an absorption band is seen at 1,466  $\text{cm}^{-1}$ . The IR spectra of bulk sodium oleate [22, 23] show absorption at 2,920 ( $d^-$ ), 2,850 ( $d^+$ ), 1,555 ( $\text{COO}^-$  (asym)) and 1,440 ( $\text{COO}^-$  (sym))  $\text{cm}^{-1}$ . So the absorption at 1,466  $\text{cm}^{-1}$  can be attributed to the presence of carboxylic ( $\text{COO}^-$ ) group. For the monolayer there is a shift in the absorption band of  $-\text{COO}^-$  (sym) by 26  $\text{cm}^{-1}$  from that of the bulk sample in the direction of higher frequency. This shift indicates the formation of new chemical species on steel [22, 23].

The intensity of absorption bands depends on the concentration and the orientation of molecules on the surface. The absence of a band at 1,555  $\text{cm}^{-1}$ — $\text{COO}^-$  (asym) indicates that the axis of the carboxyl group is anchored on the steel surface and is directed near normal to the surface [22, 23]. The packing density of the self-assembled monolayer is indicated by the FWHM (full width at half maxima). Here the FWHM for the methylene group is found to be 18.5  $\text{cm}^{-1}$ , which indicates that a reasonably closed packed monolayer has formed [31].



**Fig. 1** FTIR spectra of sodium oleate on steel (roughness 3–4 nm rms), deposition time = 20 h



**Fig. 2** Friction force versus normal load of sodium oleate deposited on steel (substrate roughness = 3–4 nm rms) obtained by lateral force microscopy. Sliding speed = 200 nm/s. 0% Relative humidity (RH) environment. Effect of loading (–8 nN to 40 nN) and unloading from 40 nN normal load on friction

Figure 2 shows the friction of the SAM to increase nonlinearly with load to reach a peak of about 8 nN at 17 nN normal load and then to decline with increasing load to a value of about 4–5 nN when the normal load is in the 30–40 nN regime. When the SAM is unloaded from about 40 nN normal load the loading path is not retraced and an almost linear unloading path, where the friction force is almost linearly proportional to the normal load, is followed through a low-friction regime. Taking this path to be linear gives a coefficient of friction of about 0.08, a value cited by Bowden and Tabor [30] for fatty soaps formed on metallic substrates. Figure 3 shows the friction recording in a typical loading cycle to a peak load of 18 nN (peak friction). Here the loading path is retraced on unloading. A normal load of 17–18 nN thus appears to be the threshold load, which marks the transition from where the friction path is reversible to where it is irreversible.

Taking up the friction path; –8 nN to 35 nN followed by 35 nN to –8 nN first, the path may represent a large hysteresis loop. If that is so reloading the same scan area should generate the bell-shaped path. Alternatively if a new interface material is manufactured in the 17–35 nN loading range, reloading the same scan area should retrace the low-friction characteristic observed in the unloading path of the first cycle. To clarify this we scanned the area slid in the first cycle (0 to 35 to –8 nN) repeatedly using the same loading cycle. The friction in the second and subsequent scans never followed the original bell-shaped curve and remained always at the low level, a level similar to that obtained in the unloading part of the first cycle of loading. A small magnitude of friction hysteresis was observed in these ‘subsequent’ loading cycles, Fig. 3b shows the friction recording of a cyclic scan 2 (–8 to 35 nN) of the area which has been cyclically scanned initially (scan 1) to a peak load

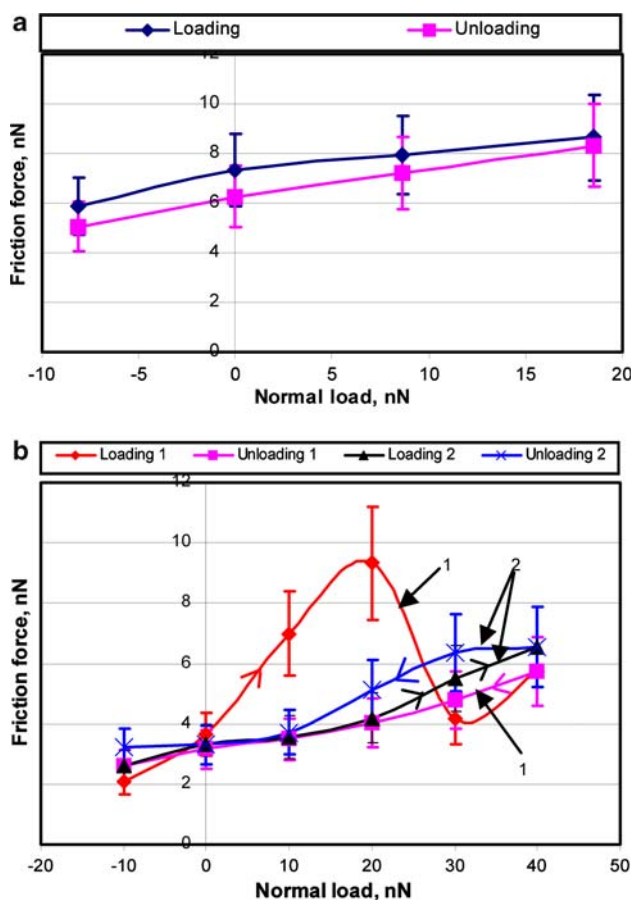


**Fig. 3** (a) A typical friction force recording, loading to maximum friction and unloading back to  $-8$  nN load. Sliding velocity =  $200$  nm/s.  $0\%$  RH, Lateral force microscopy, Substrate roughness =  $3\text{--}4$  nm rms. (b) Effect of Cyclic loading on friction force (Normal load  $\sim -8$  to  $35$  nN). Cycle 1 is sliding of pristine monolayer; cycle 2 is sliding of scan area (track) generated in cycle 1

of  $35$  nN. We infer that a new interface material is generated, most probably by chemical interaction between the SAM and the interface in the first cycle of loading to a peak load of  $35$  nN. In subsequent scans of the same track we record the friction of the new interface material. The bell-shaped nature of the friction characteristic with respect to load was also observed (Fig. 4) when the experiments were conducted in a nanotribometer using a  $2$  mm steel ball sliding on the SAM assembled on a steel substrate. The high coefficient of friction ( $0.3\text{--}0.4$ ) recorded in nanotribometer test, compared to that observed in the LFM experiment is very likely due to the fact that the rough ( $4\text{--}5$  nm rms) steel ball in the former experiments punctured the monolayer especially at the edges of the contact, establishing solid–solid contact. Unlike in the case of the LFM experiments, in nanotribometer experiments broken lines, parallel to the sliding direction, appeared at the edge of contact.

To put the results in a lubrication perspective we performed LFM experiments on a clean (see Sect. 2.1) bare

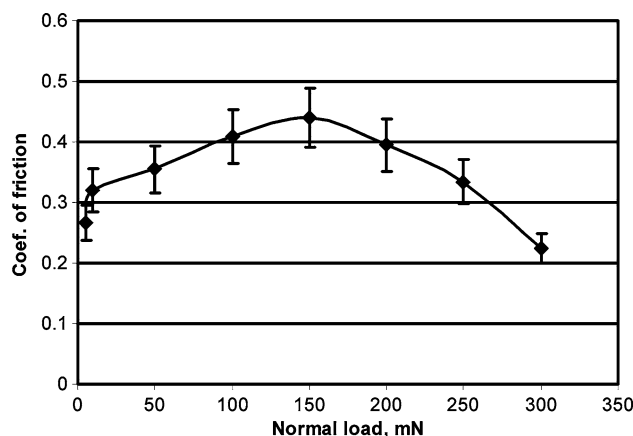


**Fig. 4** Variation of coefficient of friction with normal load obtained by nanotribometry.  $2$  mm diameter steel ball (roughness =  $3\text{--}4$  nm rms) substrate stainless steel (roughness =  $4\text{--}5$  nm rms), sliding speed =  $5$  mm/s,  $0\%$  RH

steel surface at  $30\%$  relative humidity (RH). Figure 6 shows a zero load friction force of about  $5$  nN and near linear, near reversible and monotonic changes in friction force in the  $0\text{--}50$  nN normal load regime, registering a friction coefficient of about  $1.0$ . This friction coefficient is high compared to what is achieved when the steel substrate carries an oleate monolayer. In the later case coefficient of friction of  $0.3$  is achieved in the  $0\text{--}17$  nN (normal load) regime in the first loading cycle and  $0.08$  is achieved in all subsequent load cycles (Fig. 3b).

Taking up next the friction path generated in the first cycle in the  $-8$  to  $17$  nN load range, we first note the monotonic increase in friction force with increasing load and the retracibility of the loading path on unloading. Such characteristics have been reported [3, 4, 12, 13, 32] for a variety of surfactants deposited on relatively passive surfaces such as silicon and mica. This behavior indicates that loading to  $17$  nN has not brought about any permanent change in the pristine monolayer, which recovers its original physical and chemical states after cyclic loading. The friction force  $F$  may be written as  $F = \tau^* A$ , where  $\tau^*$  is the interfacial shear strength and ‘ $A$ ’ is the contact area. We measured the pull-off force between the AFM tip ( $\text{Si}_3\text{N}_4$ , tip radius  $\approx 30$  nm) and the SAM at  $30\%$  relative humidity and estimate the work of adhesion to be  $10$  mJ/m<sup>2</sup>. The contact area ‘ $A$ ’ using the JKR model (Johnson, Kendall and Robert, [33]) is estimated to increase from  $707$  to  $873$  nm<sup>2</sup> (the reduced modulus is  $1.3$  GPa [34]) due to an increase in normal load from  $0$  to  $17$  nN. The corresponding increase in  $\tau^*$  is from  $5$  to  $12$  MPa. Thus the interfacial shear stress and the contact area, both increase with increasing normal load and contribute to the positive gradient of the friction force with load, in the  $0\text{--}17$  nN range. Previous experimental [27, 29, 32] and simulation studies [17, 28] have suggested that

increasing the normal load enhances conformational changes in the self-assembled organic molecules. This leads to the generation of greater avenues of energy dissipation. There is a consequent increase in the friction force with normal load. The conformational changes (except at very high loads [29]) are reversible and lead to retracing of the loading path on unloading. The positive gradient of the friction path in the 0–17 nN load range may therefore be attributed at least partially to reversible conformational changes.

An observation which is repeatable and interesting, but for which, we have no adequate explanation, is the effect of substrate roughness on the friction of oleate SAM on steel. Figures 5 and 6 show the effect of lowering substrate

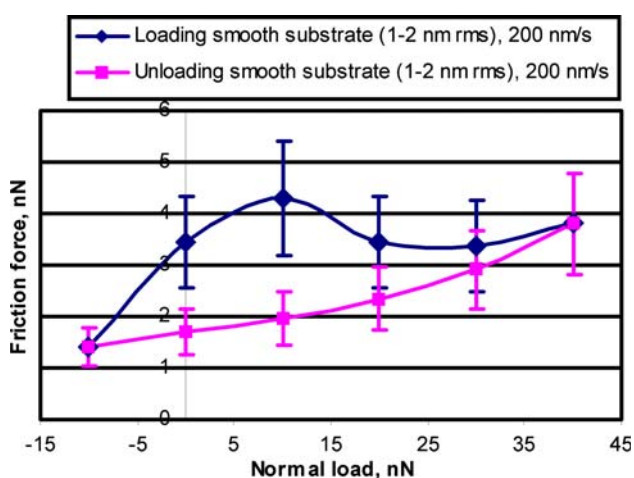


**Fig. 5** Friction force versus normal load of sodium oleate deposited on steel (substrate roughness = 1–2 nm rms) obtained by lateral force microscopy. Sliding speed = 200 nm/s. 0% Relative humidity (RH) environment. Effect of loading (–8 nN to 40 nN) and unloading from 40 nN normal load on friction

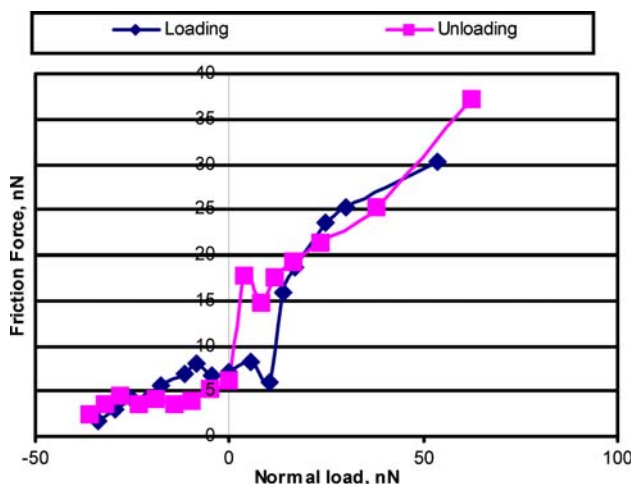


**Fig. 6** Friction force of bare steel, substrate roughness = 3–4 nm rms, 0% RH, Lateral force microscopy, sliding speed = 200 nm/s

roughness on the near cyclic friction path of sodium oleate SAM. To do this experiment the steel surface was milled by Focused Ion Beam (FIB) to generate a rms roughness of 1–2 nm. Figure 5 shows that the trend in friction (LFM) with load for a smooth substrate is similar to that obtained (Fig. 2) when the experiment was done on a rough surface. Making the surface smoother lowers; (1) the level of friction force in the part of the cycle where this force has a positive gradient, (2) the normal load at which the peak friction occurs and (3) the friction forces recorded in the unloading part of the cycle. FTIR spectra we have recorded for SAMS deposited on substrates of different roughnesses show an increase in packing density but no change in the conformational order, when the substrate is made smoother. It is also known [35] that an increase in packing density lowers friction in nanotribological experiments. This may explain why in the first part of the loading cycle where the friction has a positive gradient with load, the oleate SAM on a smooth surface registers lower friction than when it is deposited on a rough surface.

In the unloading part of the loading (maximum load = 35 nN) cycle the SAM, we argue above, is transformed to a low-friction film. The film is likely to smear the substrate. The shear strength,  $\tau^*$ , of this film should not change with roughness. The real contact area ‘ $A_r$ ’ of the film when on a smooth surface is however higher than when it is smeared on a rough surface [36]. The friction  $F = \tau^* A_r$  corresponding to the smooth substrate may thus be expected to be higher than when the substrate is rough. This is contrary to what we observe experimentally. We have no adequate explanation at present for the roughness effect.

The results presented here suggests that when a pristine SAM is slid, the frictional response upto a critical contact pressure is due to physical changes (which is of course reversible on unloading) in the molecular assembly. At pressures greater than the critical pressure, the frictional response is that of a new material. We suggest that this new material is created when the molecules are brought into close proximity of the steel substrate at high pressures and slid under these pressures. Under this condition chemical bonds may form between the molecular backbones and the steel to generate this low-friction interface material. While we have not yet characterized this material, the characteristic low order of observed friction suggests that it is a fatty soap.

## 4 Conclusions

Friction force microscopy at 0% relative humidity of sodium oleate self-assembled on steel revealed the existence of peak friction in a bell-shaped friction-load characteristic. The frictional path with normal load up to

the peak friction load is retracable on unloading while that at higher loads the frictional change is permanent. Based on this we conclude that a new low-friction film is formed when the SAM is slid under high load.

**Acknowledgments** The authors are grateful to the Bharat Petroleum Corporation Ltd. (BPCL) for the financial grant, which has made this work possible. They also acknowledge the help of Ms. Geetha, Ms. Savitha, Ms. Bindu, and Mr. H. S. Shamasunder for carrying out this work. They acknowledge the useful discussion they had with Prof. Roland Bennewitz of McGill University in preparing the manuscript.

## References

- Burnham, N.A., Dominguez, D.D., Mowery, R.L., Colton, R.J.: Probing the surface forces of monolayer films with an atomic-force microscope. *Phys. Rev. Lett.* **64**(16), 1931–1934 (1990)
- Overney, R.M., Takano, H., Fujihira, M., Paulus, W., Ringsdorf, H.: Antisotropy in friction molecular stick-slip motion. *Phys. Rev. Lett.* **72**(22), 3546–3549 (1994)
- Liu, Y., Evans, D.F., Song, Q., Grainger, D.W.: Structure and frictional properties of self-assembled surface monolayers. *Langmuir* **12**, 1235–1244 (1996)
- Bouhacina, T., Aime, J.P., Gauthier, S., Michel, D.: Tribological behavior of a polymer grafted on silylated silica probed with a nanopip. *Phys. Rev. B.* **56**(12), 7694–7703 (1997)
- Barena, E., Kopta, S., Ogletree, D.F., Charych D.H., Salmeron, M.: Relationship between friction and molecular structure: alkylsilane lubricant films under pressure. *Phys. Rev. Lett.* **82**(14), 2880–2883 (1999)
- Schonherr, H., Julius, G.V.: Tribological properties of self-assembled monolayers of fluorocarbon and hydrocarbon thiols and disulfides on Au (111) studied by scanning force microscopy. *Mat. Sci. Eng. C.* **8–9**, 243–249 (1999)
- Fujita, M., Fujihira, M.: Effect of temperature on friction observed between a Si<sub>3</sub>N<sub>4</sub> tip and dodecanethiol self-assembled monolayer on Au (111). *Ultramicroscopy* **91**, 227–230 (2002)
- Zang, Q., Archer, L.A.: Boundary lubrication and surface mobility of mixed alkylsilane self-assembled monolayers. *J. Phys. Chem. B.* **107**, 13123–13132 (2003)
- Duwez, A.S., Jonas, U., Klein, H.: Influence of molecular arrangement in self-assembled monolayers on adhesion force measured by chemical force microscopy. *Chemphyschem* **4**, 1107–1111 (2003)
- Quian, L., Tian, F., Xiao, X.: Tribological properties of self-assembled monolayers and their substrates under various humid environments. *Tribol. Lett.* **15**(3), 169–176 (2003)
- Lee, D.H., Taeyoung O., Cho, K.: Combined effect of chain length and phase state on adhesion/friction behavior of self-assembled monolayers. *J. Phys. Chem. B.* **109**, 11301–11306 (2005)
- Schirmeisen, A., Jansen, L., Holscher, H., Fuchs, H.: Temperature dependence of point contact friction on silicon. *Appl. Phys. Lett.* **88**, 123108–123111 (2006)
- Yoshizawa, H., Chen, Y.-L., Israelachvili, J.: Fundamental mechanisms of interfacial friction. 1.Relation between adhesion and friction. *J. Phys. Chem.* **97**, 4128–4140 (1993)
- Yoshizawa, H., Israelachvili, J.: Fundamental mechanisms of interfacial friction. 2.Stick-slip friction of spherical and chain molecules. *J. Phys. Chem.* **97**, 11300–11313 (1993)
- Drummond, C., Israelachvili, J., Richetti, P.: Friction between two weakly adhering boundary lubricated surfaces in water. *Phys. Rev. E.* **67**, 066110–066126 (2003)
- Ohzono, T., Fujihira, M.: Molecular dynamics simulations of friction between an ordered organic monolayer and rigid slider with an atomic-scale protuberance. *Phys. Rev. B.* **62**(24), 17055–17071 (2000)
- Zhang, L., Leng, Y., Jiang, S.: Tip-based hybrid simulation study of frictional properties of self-assembled monolayers: effects of chain length, terminal group, scan direction, and scan velocity. *Langmuir* **19**, 9742–9747 (2003)
- Urbakh, M., Klafter, J., Gourdon, D., Israelachvili, J.: The non-linear nature of friction. *Nature* **430**, 525–528 (2004)
- Glosli, J.N., McClelland, G.M.: Molecular dynamics study of sliding friction of ordered organic monolayers. *Phys. Rev. Lett.* **70**, 1960–1963 (1993)
- Kuwamura, M., Fujita, K.: Antiwear properties of lubricant additives for high silicon aluminum alloy under boundary lubrication conditions. *Wear* **89**, 99–105 (1983)
- Zhang, S.: Emerging biological materials through molecular self assembly. *Biotechnol. Adv.* **20**, 321–339 (2002)
- Rozeenfel, I.L., Loskutov, A.I., Alekseev, V.N.: Adsorption of sodium oleate and water on an oxidized aluminum surface. *Inst. Phys. Chem. Moscow* **2**, 233–237 (1982)
- Loskutov, A. I., Bratkov, A.A., Il'inskii A.A.: Interaction of sodium oleate with the surface of aluminum. *Inst. Phys. Chem. Moscow* **6**, 1140–1145 (1985)
- Devaprakasam, D., Khatri, O.P., Shankar, N., Biswas, S.K.: Boundary lubrication additives for aluminum: a journey from nano to macrotribology. *Tribol. Int.* **38**, 1022–1034 (2005)
- Schey, J. A.: Tribology in metalworking: friction, wear and lubrication, American Society for Metals (1983)
- Ivanova, I.Y., Machulski, B.M., Zhelibo, E.P., Alkeseenko, A.I.: Effect of electrolysis time on the magnetic properties of fine iron powders. *Porosh. Metallurgiya.* **2**(142), 6–11 (1983)
- Carpick R.W., Salmeron M.: Scratching the surface: fundamental investigation of tribology with atomic force microscopy. *Chem. Rev.* **97**(4), 1163 (1997)
- Tutein, A.B., Stuart, S.J., Harrison J.A.: Role of defects in compression and friction of anchored hydrocarbon chain on diamond. *Langmuir* **16**, 291–296 (2000)
- Salmeron M.: Generation of defects in model lubricant monolayers and their contribution to energy dissipation in friction. *Tribol. Lett.* **10**, (1–2), 69–79 (2001)
- Bowden, F.P., Tabor, D.: *The Friction and Lubrication of Solids*. Oxford University Press, USA (1986)
- Byrd H., Pike J.K., Talham D.R.: Inorganic monolayers formed at an organic template: a langmuir-blodgett route to monolayer and multilayer films of zirconium octadecylphosphonate. *Chem. Mater.* **5**, 709–715 (1993)
- Xiao, X., Hu, J., Charych, H., Salmeron, M.: Chain length dependence of the frictional properties of alkylsilane molecules self assembled on mica studied by atomic force microscopy. *Langmuir* **12**, 235–237 (1996)
- Maugis, D.: *Contact, Adhesion and Rupture of Elastic Solids*. Springer-Verlag Berlin Heidelberg, New York (1999)
- Khatri, O.P., Devaprakasam, D., Biswas, S.K.: Frictional responses of Octadecyltrichlorosilane (OTS) and 1H, 1H, 2H, 2H—Perfluorooctyltrichlorosilane (FOTS) monolayers self-assembled on aluminium over six orders of contact length scale. *Tribol. Lett.* **20**(3–4), 235–246 (2005)
- Khatri, O.P., Biswas, S.K.: Boundary lubrication capabilities of alkylsilane monolayer self-assembled on aluminium as investigated using FTIR spectroscopy and nanotribometry. *Surf. Sci.* **600**, 4399–4404 (2006)
- Johnson, K.L.: *Contact Mechanics*. Cambridge University Press, UK (2003)